PHYSICAL REVIEW D **94,** 054506 (2016)

Statistical tweaks and meson masses

Saumen Datta,[*] Sourendu Gupta,[†] and Anirban Lahiri[‡]
Department of Theoretical Physics, Tata Institute of Fundamental Research, Homi Bhabha Road, Mumbai 400005, India

Pushan Majumdar[§]
Department of Theoretical Physics, Indian Association for the Cultivation of Science, Raja Subodh Chandra Mallick Road, Jadavpur, Kolkata 700032, India
(Received 27 June 2016; published 13 September 2016)

We examine meson correlation functions over a large range of lattice spacing and quark mass in simulations with the standard staggered action. We find that the distribution of meson correlation functions is non-Gaussian, with long tails. We modify the statistical analysis to take care of the non-Gaussianity. Current day improvements in the statistical quality of data on hadron correlations further allow us to simplify certain aspects of the analysis of masses. We examine these changes through the analysis of pions and apply them to the vector meson. We also remark on the relation between the vector mass and flow scales.

DOI: 10.1103/PhysRevD.94.054506

I. INTRODUCTION

In any lattice computation, one needs to specify the lattice scale. The earliest approach to this was to determine a hadron mass on the lattice and use this to set the scale. The difficulty of determining hadron masses with small systematic uncertainties has gradually led to the development of other techniques. Currently the simplest seems to be the flow scale w_0 [1]. Since this is a theory scale, not measurable in experiments, it is useful to compare it with other scales and with the same scale determined using different lattice actions. Such comparisons quantify the approach to the continuum limit.

In a previous work we examined the flow scale with two flavors of rooted naive staggered quarks over a large range of lattice spacing and quark masses [2]. By comparing the flow scale with the QCD scale in the MS-bar scheme, $\Lambda_{\overline{\rm MS}}$, determined using the Lepage-Mackenzie scheme, we found that $w_0 = 0.13^{+0.01}_{-0.02}$ fm. This flow scale is smaller than those obtained using other discretizations of the Dirac operator. However, there may be UV corrections in comparing the flow scale with the QCD scale so determined, which have not been examined yet. So we examine here the ensembles generated in the earlier study to determine the vector meson mass.

This leads us to reexamine the extraction of meson masses from naive staggered quarks. The last such measurements were performed 25 years ago, when the current technology of using covariance matrices in fits was just a few years old [3]. However, computational hardware has scaled from a few hundred megaflops to a few hundred teraflops in the intervening years. As a result, one can beat down autocorrelations between configurations tremendously even with the old algorithms. With a set of almost uncorrelated configurations one may use simpler statistical tools.

Consider one of the changes possible if the sampling of lattice gauge configurations became cheap. Measurements of correlation functions could be done using completely different sets of a very large number of configurations at each distance, each drawn from a thermalized configuration. Since the measurements of correlators at each separation would then be statistically independent, the covariance between them would vanish, and it would be easier to fit masses to them. While this ideal is still out of reach, it is worth considering analyses which make it simple to transit from statistics-limited to large-statistics studies.

Our basic tool is the widely used nonparametric method called bootstrap or resampling [4]. For any statistic obtained from a configuration, we estimate its distribution nonparametrically by bootstrap. This versatile construction replaces the assumption that the statistic is Gaussian distributed. The median and the 34% limits above and below it are taken as the nonparametric estimate of the average and error. The sample median has the nice property that its distribution tends to a Gaussian. This is an old theorem, whose proof we present in the Appendix, since it seems to be relatively poorly known in lattice gauge theory [5]. Some limits on the use of bootstraps were explored in [6]. Using this for multidimensional resampling, or by nesting bootstraps, one can generate a variety of analysis tools.

We report hadron masses determined in simulations with two flavors of staggered quarks using the configurations

[*]saumen@theory.tifr.res.in
[†]sgupta@theory.tifr.res.in
[‡]anirban@theory.tifr.res.in
[§]tppm@iacs.res.in

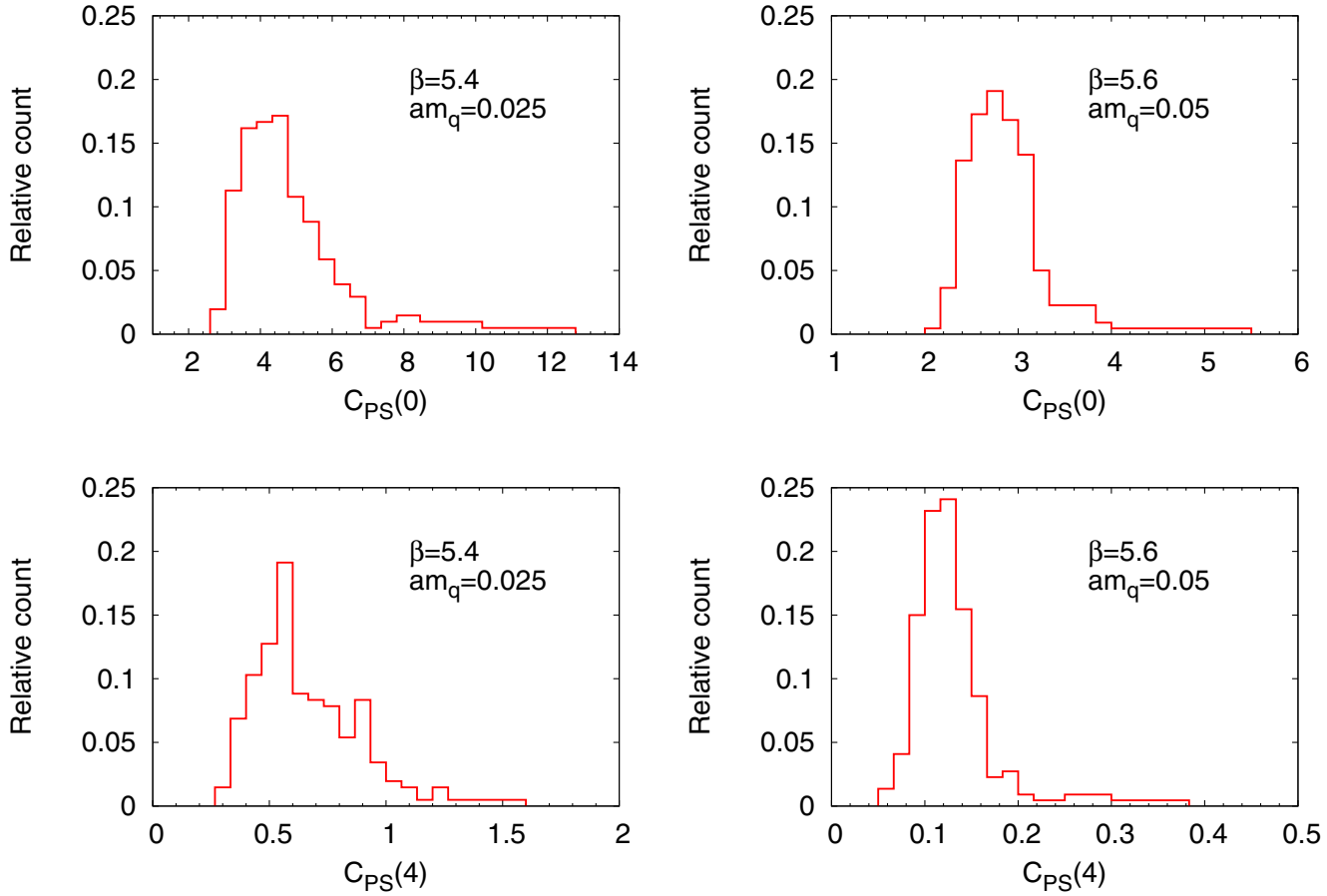

FIG. 1. The distribution of measurements of the PS correlator at distance zero for two representative run IDs 6 (left) and 14 (right). The ID numbers associated with runs are given in Table I. Such highly skewed distributions are seen to be generic.

described in [2]. Measurements of the mass of the pseudo-Goldstone pion were reported earlier using techniques similar to those described in [3]. We revisit that measurement and also report our estimates of the masses of vector mesons.

In the next section we report on an exploration of various statistical methods using staggered pseudo-Goldstone pion correlators. In the section after that we report measurements of vector meson masses. We compare the setting of scale using m_ρ and w_0 and give an estimate of w_0 from m_ρ. Our main conclusions are collected in the fourth section. In an Appendix we describe a theorem on the distribution of sample medians which is useful for bootstrap estimates of random variates which are not Gaussian distributed.

II. PIONS

The staggered pseudo-Goldstone pion is a good test bed for exploring statistical techniques for two reasons. First, because masses are typically small, the relative uncertainty in the correlation function is small. Second, unlike other staggered hadrons, there is no opposite parity channel to complicate the analysis, and it is often sufficient to use a fitting form

$$C_{\rm PS}(t) = A\cosh\left[m\left(\frac{aN_t}{2} - t\right)\right], \tag{1}$$

where a is the lattice spacing and A and ma are fit parameters, and PS denotes the pseudo-scalar meson.

We begin by examining the distribution of the measurements of the PS correlation function at fixed separation t. Two representative histograms of the measurements of the PS correlator are shown for each of $t = 0$ and $t = 4$ in Fig. 1. They are highly skewed. We found that the set of configurations which give rise to measurements in the tail of the distribution of the correlator at $t = 0$ are generically those which populate the tail at other t. Such long-tailed and skewed ensembles of the correlators are generic, in the sense that we saw such distributions for all 22 cutoffs and quark masses which we examined.

This is not an artifact of a lack of thermalization. The sequence of configurations which we used were thermalized according to global measurements like average plaquette or quark condensate. Moreover, the measurements which lie at the tails of the distribution are distributed throughout the runs and not clustered together.

TABLE I. Comparison of pion masses extracted by the two methods labeled NP and IS, whose explanations are given in the text.

ID	L/a	β	am_q	S	am_π(NP)	am_π(IS)
1	16	5.2875	0.1	50	0.7899 (27)	0.7904 (23)
2	16	5.2875	0.05	50	0.5753 (23)	0.5756 (27)
3	16	5.2875	0.025	70	0.4159 (26)	0.4161 (27)
4	16	5.2875	0.015	50	0.3241 (24)	0.3240 (34)
5	16	5.4	0.05	75	0.6033 (47)	0.6030 (54)
6	16	5.4	0.025	51	0.4376 (61)	0.4376 (71)
7	24	5.4	0.015	51	0.3500 (18)	0.3504 (21)
8	32	5.4	0.01	40	0.2922 (17)	0.2925 (12)
9	16	5.5	0.05	50	0.6184 (91)	0.6177 (93)
10	24	5.5	0.025	101	0.4463 (22)	0.4459 (22)
11	28	5.5	0.015	120	0.3542 (19)	0.3541 (21)
12	32	5.5	0.01	40	0.2896 (21)	0.2894 (30)
13	32	5.5	0.005	50	0.2129 (39)	0.2124 (43)
14	24	5.6	0.05	55	0.5938 (29)	0.5935 (27)
15	24	5.6	0.025	103	0.4255 (66)	0.4246 (78)
16	28	5.6	0.015	120	0.3299 (49)	0.3302 (56)
17	32	5.6	0.01	40	0.2682 (42)	0.2685 (44)
18	32	5.6	0.005	50	0.1973 (45)	0.1965 (30)
19	32	5.6	0.003	105	0.1506 (25)	0.1513 (24)
20	24	5.7	0.025	59	0.3954 (73)	0.3956 (59)
21	32	5.7	0.005	50	0.1751 (57)	0.1738 (55)
22	32	5.7	0.003	50	0.134 (13)	0.134 (19)

Non-Gaussian distributions of correlation functions have been sporadically reported in the literature [7]. Unlike those, the distributions which we see are not log-normal. In fact, in this case even the logarithms of correlation functions have long-tailed distributions. An extreme example is for ID number 14 (see Table I for the association of ID numbers with run parameters). For this set the distribution of $\log C_{\rm PS}(4)$, shown in the last panel in Fig. 1, has skewness -2.5 and kurtosis 25. Systematic reports of distributions of correlators is not part of the standard analysis suite of lattice gauge theory. As a result, we do not know whether our observation is of greater generality.

We investigated the configurations which give measurements in the long tail of the distribution. Pion correlation functions measured on these configurations with different source locations do not have large values of the correlator for all locations of the source. In order to understand this, it is useful to think in terms of the eigenvalue decomposition of the correlators.

Suppose that λ_i is an eigenvalue of the staggered Dirac operator, and the component of the eigenvector at site x is $|\lambda_i(x)\rangle$; then

$$D_{xy}|\lambda_i(y)\rangle = \lambda_i|\lambda_i(x)\rangle \quad \text{and} \quad D^{-1}_{xy} = \sum_i \frac{1}{\lambda_i}|\lambda_i(x)\rangle\langle\lambda_i(y)|. \tag{2}$$

As a result, any local mesonic correlation function is given by

$$C(x,y) = \sum_{ij}\frac{1}{\lambda_i\lambda_j}\langle\lambda_i(x)|\gamma|\lambda_j(x)\rangle\langle\lambda_j(y)|\gamma|\lambda_i(y)\rangle, \tag{3}$$

where γ is the spin-flavor matrix which enters the source for the meson under consideration. If a configuration has one or more eigenvalues λ_i which are very small compared to the minimum eigenvalue in a generic configuration, then the correlation function becomes large. If, at the same time, the corresponding eigenvectors are localized, then $C(x,y)$ may not be equally large for all x and y. This would imply that on these configurations some sources give much larger values of the correlator than others. Previous investigations have shown that the eigenvalues and eigenvectors have exactly this kind of behavior in the presence of topological structures [8]. This leads us to believe that topology is generally the reason for the skewed distributions which we see [9].

Since the tail of the distribution of measurements of the correlators is so long, it is not clear whether the central limit theorem applies. As a result, justification for the use of Gaussian statistics (labeled G), through the use of means, variances, and covariance matrices, is lacking. On the other hand, it is safe to use a nonparametric bootstrap analysis (labeled NP). This does have an effect on the determination of the mass, as we show in Fig. 2. There is a tendency for NP to lead to a higher mass, although, as the figure shows, the discrepancy between the two methods is generally less than a 1-σ effect.

The molecular dynamics time separation between successive stored configurations which we used are larger than

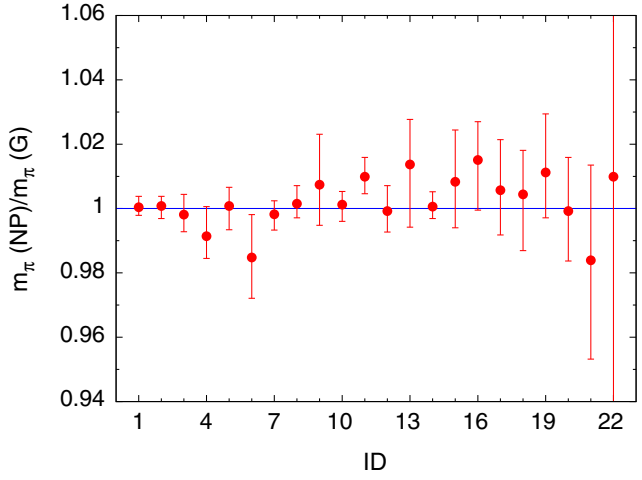

FIG. 2. The ratio of pion masses extracted with nonparametric bootstrap estimators of the correlator (labeled NP) and with Gaussian estimators (labeled G). The uncertainty in the ratio are obtained by repeating the bootstrap resampling and generating the distribution of the ratio. The ID numbers on the ordinate are associated with run parameters in Table I.

those used before for naive staggered quark simulations [3,10–12] and are typical of those used today. Additive increase of the MD time separation decreases autocorrelations exponentially. So it is worthwhile performing the analysis in which the correlation function at each distance is resampled independently.

Such a comparison is shown in the first panel in Fig. 3 for the PS correlator in one of our simulations. The ratio of the correlation function obtained through independent sampling (labeled IS) and that obtained using our usual sampling (labeled NP as before) is completely consistent with unity at all separations. This conclusion is true for all sets of simulations we have made. A comparison of the masses obtained by the two methods is shown in Fig. 3 through the ratio of the masses. As expected from the behavior shown in the first panel, the masses are not changed by the sampling of the correlator. The pion masses estimated using these two methods are collected in Table I. From the table one also sees that our exploration of statistical methods covered a very wide range of pion masses in lattice units.

Finite volume corrections for pions are larger than for other hadrons. They have been investigated in detail before [13,14]. We tried to estimate corrections using configurations generated at smaller volumes with fixed lattice spacing and quark masses. In agreement with previous results, we found that finite volume effects are not visible above statistical uncertainties when $Lm_\pi \geq 5$. The case of ID 22 deserves special mention, since $Lm_\pi = 4.2$, and one might expect as large as a 1% finite volume effect [13]. However, as shown in Table I, the statistical uncertainty in this measurement is about 10%. So finite volume effects can be uniformly neglected for all the sets of measurements.

III. THE VECTOR

On examining the distributions of other meson correlation functions, we found that they are skewed in general. We show examples for the vector correlator in Fig. 4. The tails of these distributions generally come from the same configurations as for the pion. As before, we take account of this skewness by using the methods NP and IS, explored in the previous section.

The analysis of these correlation functions is more complex than that of the pseudo-Goldstone pion because the correlator contains an oscillating staggered piece

$$C_V(t) = A\cosh\left[m\left(\frac{aN_t}{2} - t\right)\right] + (-1)^{t/a}A'\cosh\left[m'\left(\frac{aN_t}{2} - t\right)\right], \quad (4)$$

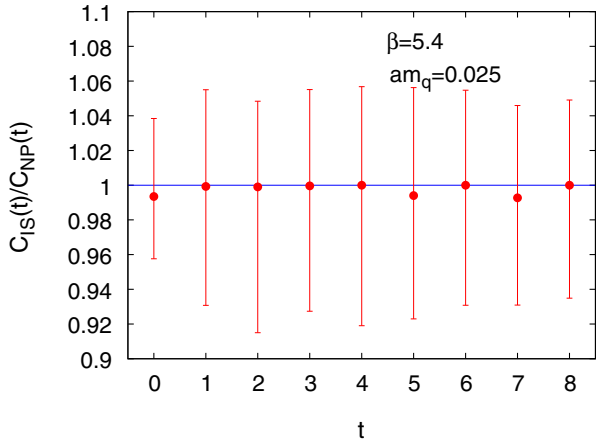

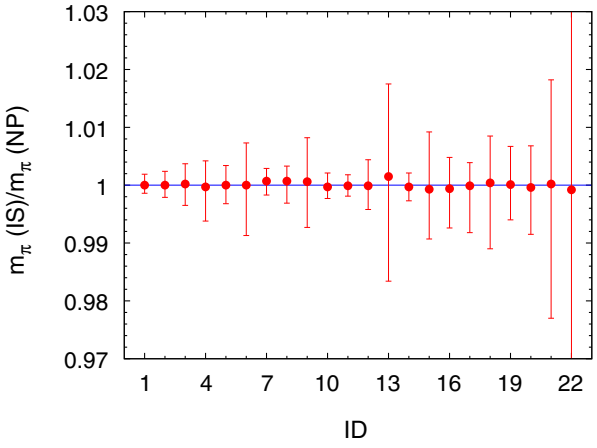

FIG. 3. The first panel shows the ratio of pion correlators extracted with independent bootstrap estimators of the correlator at each t (labeled IS) and using the same bootstrap configurations at all t (labeled NP, as before) at a representative run ID 6. The second panel shows the comparison of masses extracted from the two different estimators of the correlators.

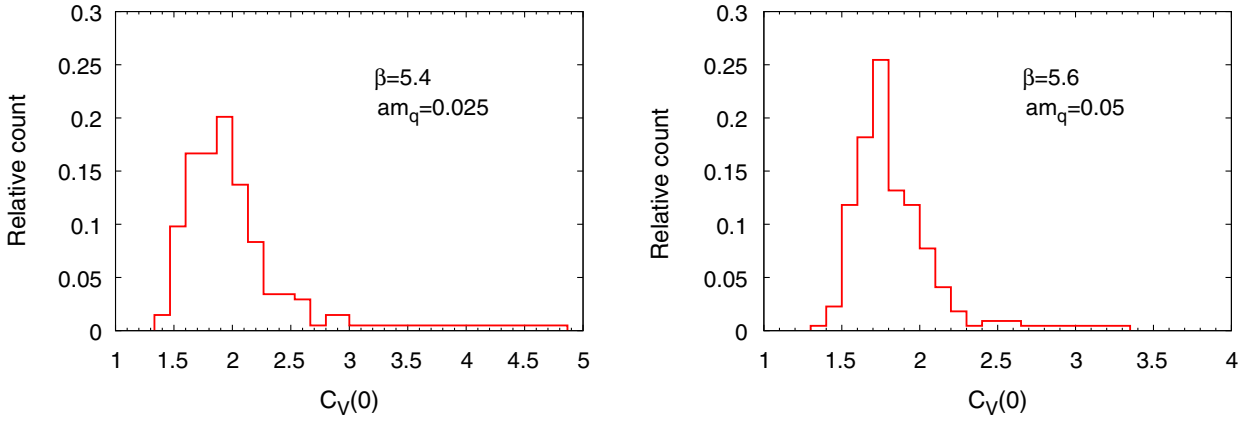

FIG. 4. The distribution of measurements of the local vector correlators at distance zero for the representative run IDs 6 and 14 seem to be non-Gaussian. The configurations which give rise to the measurements at the tail of these distributions are generally those which populate the tail of the PS correlator.

where a is the lattice spacing. We extract effective masses by using four successive values of t to extract the four parameters. We looked for plateaus in such effective masses and fitted the correlation function above within the range of the plateau. The statistical uncertainty in the fitted mass, ma, was obtained using a pair of nested bootstraps. For each set of resamplings of the correlation function, the fit returned a value of the parameters being fitted. A further bootstrap over this process gave a distribution of the parameters. This was used to estimate parameter uncertainty in the usual way.

As one can see from the local masses in Fig. 5, the region over which a fit can be performed is significantly shorter for the vector meson than for the pion. The lack of perfect overlap with the ground state limits the smallest values of t which we can use in the fit. As is visible in the figures, this is not necessarily a more stringent cutoff for vectors than for pions. However, since the vector mass is larger, the correlator falls faster, and the signal to noise ratio deteriorates, limiting the largest t which we can use. This large-t problem can be beaten only with statistics and therefore represents a hard CPU limitation. Instead, as is common in the literature, we try to use the small-t information. Since the correlator couples to a tower of states, it gets a contribution in the form in Eq. (4) from each state. Techniques for extracting ground and excited states simultaneously have been explored since the 1990s [15]. Notable developments are the use of variational methods with many different forms of the source [16] and Bayesian fitting [17].

Here we use the technically simpler alternative method which uses a fit of two (four, with staggering) masses to the effective masses. Since the number of fit parameters doubles, one has to take a sufficiently large interval in t to obtain a statistical test of the goodness of fit. We found that the full range of t could be fitted with two states. However, there are two sources of systematic uncertainties: first in choosing the t with which to associate the effective mass which is being fitted and second in the range over which the fit is performed. We vary the fit interval by one unit at each end point. We also let the effective mass be associated with every separation which was used to determine it. The maximum variation in ma obtained with these changes is quoted as a systematic uncertainty in this method.

Measures of systematic uncertainties are arbitrary, but one can check that different measures are close to each other. The simplest check which we have performed is that changing the end point by two lattice spacings does not change this estimate. A quite different check was to perform a fit using Bayesian priors for several of the higher masses and the full range of lattice spacings available, as suggested in [17]. Consistent with our finding that two states suffice for the usual fit, we find that two states remain well constrained. In particular, for a range of priors we find that the smallest mass is stable and equal to the values obtained by the standard fit. At the edge of this range, changing the priors induces changes in the best fit values by an amount which can be taken to be a systematic uncertainty. We observed that systematic uncertainties obtained in this way are comparable with those which we quote. The case of ID 20 (displayed in Fig. 5) deserves special mention, since the lattice size is a little too small to cleanly separate out the lowest and next state in the vector channel. In this case the Bayesian fit yields a systematic uncertainty which is about a third of that reported in Table II. The reason is that the last value of t is crucial for the mass determination. Only in such extreme cases do different measures of systematic uncertainty differ.

Run IDs 3, 15 and 20 of Tables I and II can be compared with previous measurements of masses reported in the literature [10–12]. In all three cases we find good agreement of previously quoted values of am_π with the results we report in Table I. We also find that the previously reported results on am_ρ are in

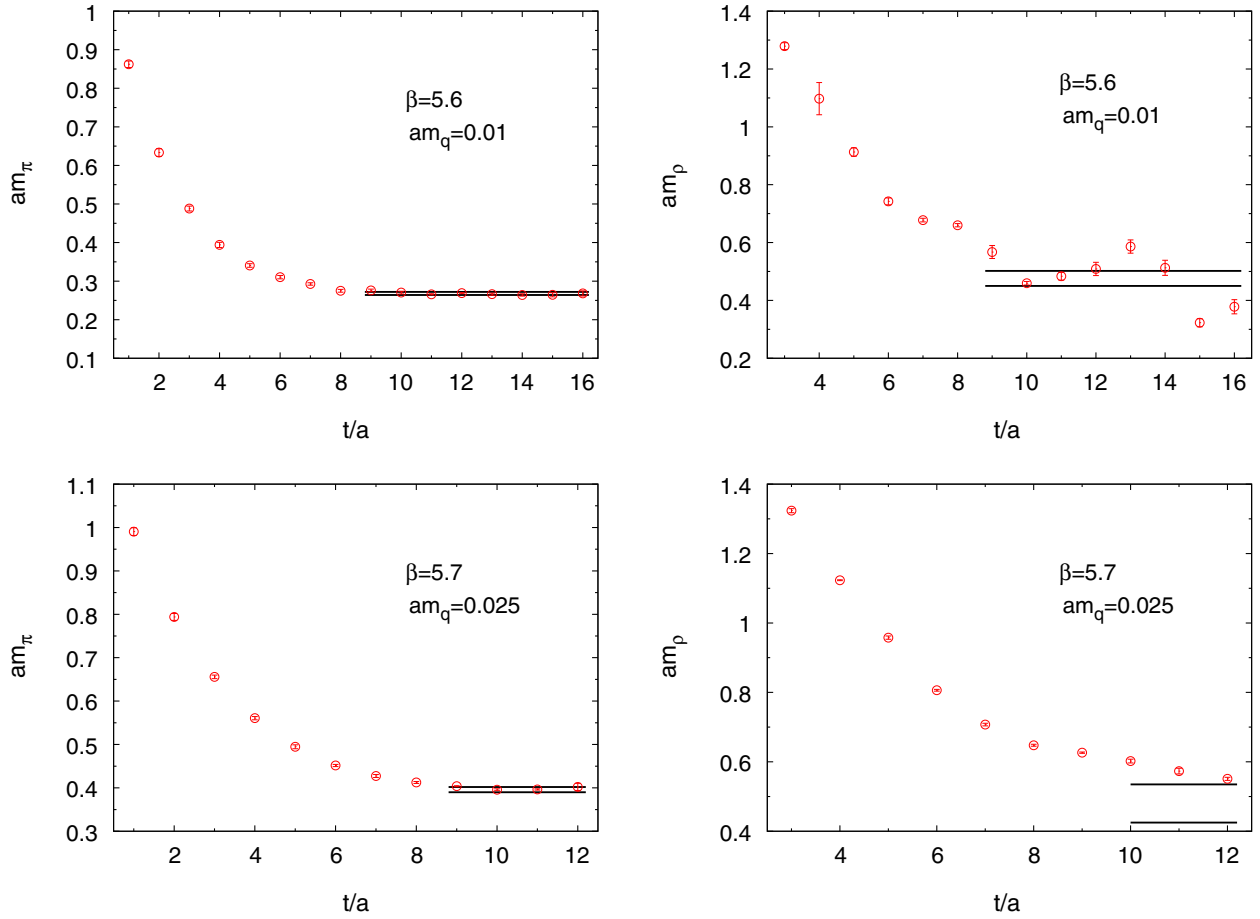

FIG. 5. Local masses for pions and vector mesons in some representative runs. The best fit masses are shown along with the local masses. For pions the band shows the 68% statistical uncertainty band. For the vector meson the band is due to the systematic uncertainties, which happen to be larger than the statistical uncertainty. For $\beta = 5.7$, am_ρ is extracted after taking into account the excited state contribution.

reasonable agreement with the vector masses we extract with single mass fits Table II.

When trying to set the lattice scale for staggered quarks, taste symmetry breaking is an issue, not only for the standard action used here but also for improved actions. A measure of taste symmetry breaking in a particle mass is

$$r = \frac{\max(|m_t - m_o|)}{m_o}, \tag{5}$$

i.e., the ratio of the spread of the masses of the taste partners of a particle, m_t, to the mass obtained from the local operator, m_o. The maximization is over all tastes. At a lattice spacing of $a \simeq 0.1$ fm, it was found that $r \simeq 0.3$ for the pion [18,19] and about 0.2 for the vector [19]. Since these ambiguities are correlated, we will take the larger value as an indicative number for the uncertainty in hadron mass scales. While it is easy to quantify taste symmetry breaking effects on masses, there is no easy measure for taste symmetry breaking effects in the measurement of w_0. Further investigation of taste symmetry ambiguities on the lattice scale is clearly required, but it lies outside the scope of this paper.

Since we have previously determined the Wilson flow scale w_0/a, we can examine our results for am_ρ also in terms of $m_\rho w_0$. In Fig. 6 we plot data on $m_\rho w_0$ as a function of $m_\pi w_0$ for the four smallest pion masses we used at the finest lattices possible. The coarsest lattice spacing among these corresponds to $a < w_0/1.7$. Since m_π^2 is proportional to a renormalized quark mass, when this is small enough, m_ρ should be linear in this. Although the uncertainties at the smallest quark masses are rather large, the data seem to fall in the range where the linear extrapolation seems reasonable. In view of this, we fitted an extrapolation function for $m_\rho w_0$ linear in terms of $(m_\pi w_0)^2$. The 68% uncertainty band on this extrapolation are also shown in Fig. 6.

The slope of the extrapolation may be captured in the quantity

$$S_\rho = 2\frac{m_\rho w_0(m_\pi w_0 = 0.4) - m_\rho w_0(m_\pi w_0 = 0.3)}{m_\rho w_0(m_\pi w_0 = 0.4) + m_\rho w_0(m_\pi w_0 = 0.3)}. \tag{6}$$

TABLE II. Comparison of vector masses extracted by the methods NP and IS, for various ID numbers. The IDs and the labels on masses have the same meanings as in Table I. In several cases the plateau in the local masses was too short to trust the single mass staggered fits, and the first excited state (and its staggered partner) was added to the fit. Data sets excluded from the table are too noisy for a stable fit.

		Single mass fit			Two masses fit	
ID	β	am_q	am_ρ(NP)	am_ρ(IS)	am_ρ(NP)	am_ρ(IS)
1	5.2875	0.1	1.464 (7)	1.462 (8)		
2	5.2875	0.05	1.336 (16)	1.340 (12)		
3	5.2875	0.025	1.289 (6)	1.288 (6)		
5	5.4	0.05	1.286 (4)	1.286 (3)		
6	5.4	0.025	1.177 (9)	1.177 (12)		
7	5.4	0.015	1.118 (6)	1.117 (6)		
9	5.5	0.05	1.046 (9)	1.044 (9)		
10	5.5	0.025	0.904 (4)	0.904 (4)		
14	5.6	0.05	0.844 (4)	0.844 (5)	0.820 (19) (4)	0.819 (17) (6)
15	5.6	0.025	0.638 (2)	0.639 (4)	0.572 (16) (71)	0.565 (28) (79)
16	5.6	0.015	0.595 (4)	0.595 (4)	0.577 (15) (14)	0.571 (11) (26)
17	5.6	0.01	0.475 (14)	0.476 (13)		
18	5.6	0.005	0.420 (18)	0.415 (18)	0.277 (39) (24)	0.291 (53) (24)
20	5.7	0.025	0.568 (3)	0.569 (5)	0.482 (28) (53)	0.480 (26) (55)
22	5.7	0.003	0.418 (11)	0.417 (8)	0.306 (36) (53)	0.304 (28) (72)

The fit shown in Fig. 6 gives $S_\rho = 0.14 \pm 0.08$. With our set of simulations we are unable to remark on the possible lattice spacing dependence of this slope. A previous estimate of the ratio $w_0/\sqrt{t_0}$ with this set of simulations showed that a smooth limit is reached at $a \simeq w_0/2$ [2]. While this could be taken as an indication that the slope parameter we have determined is close to its continuum value, it would be useful to check this in future.

With this fit we can extrapolate self-consistently to the physical m_π and there use the physical value of m_ρ to extract w_0 in physical units. We quote a statistical uncertainty in the extrapolation; this arises from the statistical uncertainty in the mass measurements. We also quote a systematic uncertainty which is the maximum difference between this extrapolation and the two obtained by leaving out of the fits either the measurement at the smallest or the largest m_π. This gives $w_0 = 0.14 \pm 0.02 \pm 0.01 \pm 0.04$ fm, where the first uncertainty is statistical, the second is from the extrapolation to physical quark masses, and the third is from extrapolation to the continuum limit, assuming that this is dominated by taste symmetry breaking effects. This extraction of the scale w_0 is subject to the same caveats as the computations of the slope parameter S_ρ.

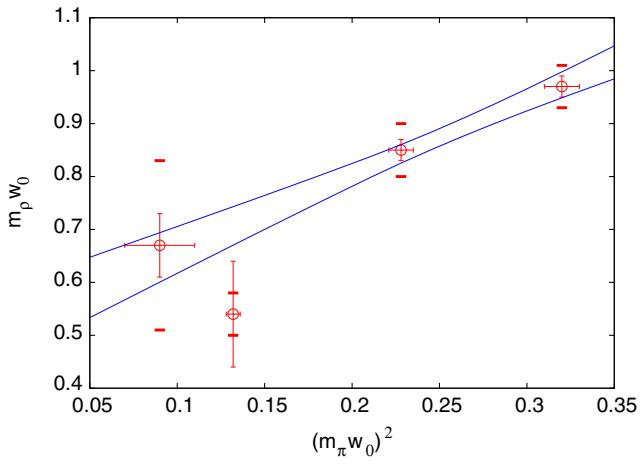

FIG. 6. $m_\rho w_0$ as a function of $(m_\pi w_0)^2$. The fat bars show systematic uncertainties; thin for statistical uncertainty. The 68% uncertainty band of a linear extrapolation fitted to the four data points is shown here.

IV. CONCLUSIONS

In Sec. II we have reported extensively on the statistical analysis of masses. We observed that the distributions of correlation functions are strongly skewed, and a Gaussian analysis of the sample cannot be justified. We found that bootstrap estimates, which do not assume any particular form of the distribution function, of the correlation functions and their uncertainties give sensible results. We are not aware of earlier systematic reports on the distribution of measurements of correlation functions. We found that the masses obtained through independent bootstrap sampling of the correlator at each t (called IS here) give results in complete agreement with sampling at all t together (which we called NP). This is shown by the detailed compilation of results in Tables I and II.

The basic results we report in this paper are collected in Table III. The measurements of w_0 were reported in [2]; they are included here for completeness. The pion and rho masses reported here are obtained using the IS sampling technique. Where older results [3,10–12] are available, they agree with ours within statistical uncertainties. Our results

TABLE III. A summary of our scale setting measurements. The scale setting by w_0 was reported in [2]. We have updated the pion masses presented in that study by reporting here the results of the analysis technique IS. For m_ρ the statistical uncertainty is given before the systematic uncertainty.

β	ma	N_s L/a	Machine	Traj (MD)	Statistics $T_0 + T \times N$	w_0/a	am_π	am_ρ	$m_\pi w_0$	$m_\rho w_0$
5.2875	0.1	16	V	1	$400 + 10 \times 50$	0.6112 (4)	0.790 (2)	1.462 (8) (7)	0.483 (1)	0.894 (5) (4)
	0.05	16	V	1	$780 + 10 \times 50$	0.6354 (6)	0.576 (3)	1.340 (12) (7)	0.366 (2)	0.851 (8) (4)
	0.025	16	V	1	$200 + 15 \times 70$	0.6539 (1)	0.416 (3)	1.288 (6)	0.2714 (13)	0.842 (4)
	0.015	16	V	1	$400 + 10 \times 50$	0.6608 (5)	0.324 (3)	⋯	0.214 (2)	⋯
5.4	0.05	16	V	2	$200 + 20 \times 75$	0.8418 (14)	0.603 (5)	1.286 (3) (2)	0.508 (4)	1.082 (3) (2)
	0.025	16	V	1	$400 + 10 \times 51$	0.9264 (21)	0.438 (7)	1.177 (12) (23)	0.406 (6)	1.09 (1) (2)
	0.015	24	V	2	$400 + 10 \times 50$	0.9600 (9)	0.354 (2)	1.117 (6) (10)	0.340 (2)	1.072 (6) (10)
	0.01	32	G	2	$200 + 20 \times 40$	0.9922 (7)	0.292 (1)	⋯	0.290 (1)	⋯
5.5	0.05	16	V	1	$200 + 20 \times 50$	1.1689 (40)	0.618 (9)	1.044 (9) (88)	0.72 (1)	1.22 (1) (10)
	0.025	24	V	1	$1680 + 10 \times 101$	1.2651 (18)	0.446 (2)	0.904 (4) (11)	0.564 (3)	1.144 (5) (14)
	0.015	28	G	2	$400 + 10 \times 120$	1.3302 (13)	0.354 (2)	⋯	0.471 (3)	⋯
	0.01	32	G	2	$200 + 20 \times 40$	1.3771 (16)	0.289 (3)	⋯	0.398 (4)	⋯
	0.005	32	BG	1	$250 + 10 \times 50$	1.4254 (37)	0.212 (4)	⋯	0.302 (6)	⋯
5.6	0.05	24	V	1	$400 + 10 \times 55$	1.4850 (26)	0.594 (3)	0.819 (17) (6)	0.882 (5)	1.22 (2) (1)
	0.025	24	V	1	$1700 + 10 \times 48$	1.6007 (33)	0.425 (8)	0.565 (28) (79)	0.68 (1)	0.90 (4) (13)
	0.015	28	G	2	$400 + 10 \times 120$	1.7087 (25)	0.330 (6)	0.571 (11) (26)	0.56 (1)	0.97 (2) (4)
	0.01	32	G	2	$200 + 20 \times 40$	1.7814 (36)	0.268 (4)	0.476 (13) (26)	0.477 (7)	0.85 (2) (5)
	0.005	32	BG	1	$300 + 10 \times 50$	1.8547 (71)	0.196 (3)	0.291 (53) (24)	0.363 (6)	0.54 (10) (4)
	0.003	32	BG	1	$600 + 5 \times 105$	1.8824 (32)	0.151 (2)	⋯	0.284 (4)	⋯
5.7	0.025	24	V	1	$530 + 10 \times 59$	1.9645 (48)	0.396 (5)	0.480 (26) (55)	0.78 (1)	0.94 (5) (11)
	0.005	32	BG	1	$370 + 10 \times 50$	2.1470 (73)	0.174 (5)	⋯	0.37 (1)	⋯
	0.003	32	BG	1	$300 + 10 \times 50$	2.2103 (162)	0.13 (2)	0.304 (28) (72)	0.30 (4)	0.67 (6) (16)

cover a wider range of lattice spacing and renormalized quark mass than was available for $N_f = 2$ naive staggered quarks earlier. Our best estimate of the slope of the rho mass with the pion mass is

$$S_\rho = 0.14 \pm 0.08, \tag{7}$$

where S_ρ is defined in Eq. (6).

Since we have earlier determined the scale w_0/a at these bare parameters, we can now use these mass measurements to estimate the scale w_0 from the vector meson mass. Extrapolation to the physical pion mass yields the value

$$w_0 = 0.14 \pm 0.02 \pm 0.01 \pm 0.04 \text{ fm}, \tag{8}$$

where the first uncertainty is due to statistical uncertainties in the extraction of masses, the second is from an estimate of the uncertainty in the extrapolation to physical pion mass and the third is an estimate of the uncertainty in the extrapolation to the continuum limit, which is dominated by taste symmetry breaking effects in the staggered pion mass. We note that systematic uncertainties from taste symmetry breaking effects may introduce further systematic uncertainties. This value for $N_f = 2$ naive staggered quarks should be compared to the value $w_0 = 0.13^{+0.01}_{-0.02}$ fm, obtained earlier by a comparison with scale setting using the Lepage-Mackenzie method for the extraction of $\Lambda_{\overline{\text{MS}}}$ (errors are statistical) [2]. Since the earlier extraction could require better control of UV artifacts than available at present, the current extraction, using a long-distance measurement, is an useful alternative method, although at present it suffers from various remaining uncertainties. It would be interesting to verify this estimate using other scales in future.

We also point out that an extraction of w_0 for $N_f = 2$ clover quarks using f_K to set the scale yields a larger value, namely $w_0 = 0.1757 \pm 0.0013$ fm, where the uncertainty is statistical [20]. While the difference is not large or statistically very significant, it is intriguing. Tracing the source of this difference will certainly allow us to understand the continuum limits of various fermion measurements better.

APPENDIX: DISTRIBUTION OF SAMPLE MEDIANS

Suppose r is a real random variate with distribution $f(r)$, and let μ be the population median. The cumulative distribution of r is

$$F(r) = \int_{-\infty}^{r} f(t)dt, \tag{A1}$$

where $F(\infty) = 1$, $F(-\infty) = 0$, and $F(\mu) = 1/2$. If we draw $2n + 1$ samples from the population and find that the

median of the sample is z, then the probability of this being so is

$$g(z) = \binom{2n+1}{n}\{F(z)[1-F(z)]\}^n f(z). \quad \text{(A2)}$$

When n is large enough, we expect z to be close enough to μ so that the Taylor expansion

$$F(z) = \frac{1}{2} + f(\mu)(z-\mu) + \frac{1}{2}f'(\mu)(z-\mu)^2 + \ldots \quad \text{(A3)}$$

converges sufficiently quickly. Then, using Stirling's approximation in the binomial coefficient, we find that

$$\log g(z) \simeq -4n[f(\mu)]^2(z-\mu)^2 + \ldots. \quad \text{(A4)}$$

This proves that $g(z)$ is Gaussian with mean μ and a variance of $1/(8n[f(\mu)]^2)$. The uncertainty in the estimate of μ therefore decreases as $1/\sqrt{n}$. This result is attributed to Laplace [21]. The proof given here is an adaptation of one from [22].

This construction fails when $f(\mu) = 0$. Then, retaining the next term in the expansion, one can prove that $g(z)$ is even narrower. Such constructions fail completely when $f(r)$ vanishes identically in a region around $r = \mu$, so that a Taylor expansion of Eq. (A3) is impossible. However, this class of probability densities is different than that for which the central limit theorem fails. An instructive example with such a pathology is

$$f(r) = \frac{1}{2}[\delta(r) + \delta(r-1)]. \quad \text{(A5)}$$

[1] For reviews, see R. Sommer, *Proc. Sci.*, LATTICE2013 (2014) 015 [arXiv:1401.3270]; R. Sommer and U. Wolff, Nucl. Part. Phys. Proc. **261–262**, 155 (2015).

[2] S. Datta, S. Gupta, A. Lahiri, A. Lytle, and P. Majumdar, Phys. Rev. D **92**, 094509 (2015).

[3] T. A. DeGrand and C. E. DeTar, Phys. Rev. D **34**, 2469 (1986).

[4] B. Efron, *The Jackknife, the Bootstrap and Other Resampling Plans*, SIAM Monograph on Applied Mathematics (Society for Industrial and Applied Mathematics, Philadelphia, 1982).

[5] Among the exceptions is A. Borici, Nucl. Phys. B, Proc. Suppl. **129–130**, 817 (2004).

[6] S. Gupta, N. Karthik, and P. Majumdar, Phys. Rev. D **90**, 034001 (2014).

[7] M. G. Endres *et al.*, *Proc. Sci.*, LATTICE2011 (2011) 017 [arXiv:1112.4023]; E. B. Gregory, A. C. Irving, C. M. Richards, and C. McNeile, Phys. Rev. D **86**, 014504 (2012); T. DeGrand, Phys. Rev. D **86**, 014512 (2012).

[8] R. V. Gavai, S. Gupta, and R. Lacaze, Phys. Rev. D **77**, 114506 (2008); T. G. Kovacs and F. Pittier, Phys. Rev. Lett. **105**, 192001 (2010); V. Dick, F. Karsch, E. Laermann, S. Mukherjee, and S. Sharma, Phys. Rev. D **91**, 094504 (2015).

[9] One other interesting conclusion from Eq. (3) is worth mentioning. Interchanging x and y in the meson correlator while simultaneously interchanging the dummy indices i and j shows that in each configuration $C(x,y) = C(y,x)$. Truncation of the summation due to incomplete convergence of the Dirac operator does not spoil this property nor does loss of arithmetic precision in one or more eigenvectors.

[10] S. Gottlieb, W. Liu, R. L. Renken, R. L. Sugar, and D. Toussaint, Phys. Rev. D **38**, 2245 (1988).

[11] K. M. Bitar *et al.*, Phys. Rev. D **42**, 3794 (1990).

[12] F. R. Brown, F. P. Butler, H. Chen, N. H. Christ, Z. Dong, W. Schaffer, L. I. Unger, and A. Vaccarino, Phys. Rev. Lett. **67**, 1062 (1991).

[13] G. Colangelo, S. Dürr, and C. Haefeli, Nucl. Phys. **B721**, 136 (2005).

[14] M. Guagnelli, K. Jansen, F. Palombi, R. Petronzio, A. Shindler, and I. Wetzorke (Zeuthen–Rome (ZeRo) Collaboration), Phys. Lett. **B 597**, 216 (2004).

[15] Y. Iwasaki *et al.*, Nucl. Phys. B, Proc. Suppl. **30**, 397 (1993); S. M. Catterall, F. R. Devlin, I. T. Drummond, and R. R. Horgan, Phys. Lett. B **321**, 246 (1994); D. Chen *et al.*, Nucl. Phys. Proc. Suppl. **47**, 382 (1996).

[16] C. Michael, Nucl. Phys. **B 259**, 58 (1985); M. Luscher and U. Wolff, Nucl. Phys. **B 339**, 222 (1990).

[17] D. Makovoz, Nucl. Phys. B, Proc. Suppl. **53**, 246 (1997); G. P. Lepage, B. Clark, C. T. H. Davies, K. Hornbostel, P. B. Mackenzie, C. Morningstar, and H. Trottier, Nucl. Phys. B, Proc. Suppl. **106–107**, 12 (2002); C. Morningstar, Nucl. Phys. B, Proc. Suppl. **109A**, 185 (2002).

[18] T. Bae, D. H. Adams, C. Jung, H.-J. Kim, J. Kim, K. Kim, W. Lee, and S. R. Sharpe, Phys. Rev. D **77**, 094508 (2008).

[19] N. Karthik (private communication).

[20] M. Bruno and R. Sommer, *Proc. Sci.*, LATTICE2013 (2014) 321 [arXiv:1311.5585].

[21] S. M. Stigler, Biometrika **60**, 439 (1973).

[22] A. Merberg and S. J. Miller, in https://web.williams.edu/Mathematics/sjmiller/public_html/BrownClasses/162/Handouts/MedianThm04.pdf.